Journal of Nuclear Medicine, published on August 12, 2021 as doi:10.2967/jnumed.121.262471

BRIEF COMMUNICATION:

The Influence of Specific Activity on the Biodistribution of ^{18}F-rhPSMA-7.3: A Retrospective Analysis of Clinical Positron Emission Tomography Data

Thomas Langbein[1], Alexander Wurzer[2], Andrei Gafita[1,3], Andrew Robertson[1], Hui Wang[1], Ayça Arçay[1,4], Michael Herz[1], Hans-Juergen Wester[2], Wolfgang A Weber[1], and Matthias Eiber[1]

[1]Technical University of Munich, School of Medicine, Klinikum rechts der Isar, Department of Nuclear Medicine, Munich, Germany

[2]Technical University of Munich, Chair of Pharmaceutical Radiochemistry, Garching, Germany

[3]Ahmanson Translational Theranostics Division, Department of Molecular & Medical Pharmacology, University of California Los Angeles, CA, USA

[4]Akdeniz University, Department of Nuclear Medicine, Antalya, Turkey

First and Corresponding Author: Thomas Langbein, MD, Klinikum rechts der Isar, Ismaninger Straße 22, 81675 Munich, GERMANY, Phone +49.89.4140.2972, Fax +49.89.4140. 4950, Email thomas.langbein@tum.de

Running title: Specific activity and ^{18}F-rhPSMA-7.3 uptake

Word count: 2554

ABSTRACT

We investigated whether the time between synthesis and injection and the resulting decrease in specific activity affects the normal organ and tumor uptake of the PSMA ligand, ^{18}F-rhPSMA-7.3, in patients with prostate cancer. **Methods:** The biodistribution of ^{18}F-rhPSMA-7.3 on PET/CT scans performed with a high specific activity (median=178.9MBq/µg, n=42) and a low specific activity (median=19.3MBq/µg, n=42) were compared. **Results:** Tracer uptake by the parotid gland, submandibular gland and spleen was moderately, but significantly lower in the "low specific activity" group than in the "high specific activity" group (median SUV_{mean} 16.7 vs. 19.2; 18.1 vs. 22.3, and 7.8 vs. 9.6, respectively). No other statistically significant differences were found for normal organs or tumor lesions. **Conclusion**: A 10-fold decrease in specific activity has only minor effects on the biodistribution of ^{18}F-rhPSMA-7.3. These findings suggest that ^{18}F-labeled PSMA ligands can be centrally produced and shipped to PET clinics in a similar way to ^{18}F-fluorodeoxyglucose.

Keywords: PSMA, PET/CT, biodistribution, molar activity, ^{18}F

INTRODUCTION

Several ^{18}F-labeled prostate-specific membrane antigen (PSMA) ligands are currently in clinical development for imaging of patients with prostate cancer (*1-3*). In the future, it is envisioned that these ligands will be produced by central radiopharmacies in batch sizes similar to ^{18}F-fluorodeoxyglucose and shipped to positron emission tomography (PET) clinics. In such a setting radioactive decay will lead to a continuous decrease of the specific activity of the PSMA ligands. This decrease in specific activity could, in principle, lead to lower tumor uptake, since the ^{18}F-labeled PSMA ligands compete with the non-labeled PSMA ligands for binding to the limited number PSMA molecules. Such a saturation of tracer uptake by a non-radioactive precursor does not occur for fluorodeoxyglucose because fluorodeoxyglucose follows the flow of glucose, which is present at orders of magnitude higher concentrations.

^{18}F-rhPSMA-7.3 represents the lead compound in a class of radiohybrid PSMA (rhPSMA) ligands which can be labelled with ^{18}F for imaging, but also with radiometals for therapeutic use (*4*). ^{18}F-rhPSMA-7.3 is a single diastereoisomer form of ^{18}F-rhPSMA-7, for which promising preliminary imaging data have been reported (*5,6*). Two multicenter, phase III trials are in progress to investigate the diagnostic accuracy of ^{18}F-rhPSMA-7.3 in primary staging (NCT04186819) and recurrence (NCT04186845) of prostate cancer.

Preclinical investigations have shown that the biodistribution of ^{18}F-labelled PSMA ligands in mice is significantly affected by the specific activity with a decreased uptake in tumor lesions and salivary glands at lower specific activities (*7*). The present study explored whether such effects also occur in humans over the range of specific activities typically injected for PSMA PET/CT studies.

MATERIAL AND METHODS

Study Design

We retrospectively reviewed data from patients who underwent ^{18}F-rhPSMA-7.3 PET/CT at our institution between August 2018 and October 2019 (Supplementary Figure 1). All reported investigations were conducted in accordance with the Helsinki Declaration and with national regulations. The retrospective analysis was approved by the Ethics Committee of the Technical University Munich (permit 290/18S) and the requirement to obtain informed consent was waived. ^{18}F-rhPSMA-7.3 administration complied with The German Medicinal Products Act, AMG §13 2b, and the responsible regulatory body (Government of Oberbayern).

^{18}F-rhPSMA-7.3 Synthesis, Administration and Image Acquisition

^{18}F-rhPSMA-7.3 was synthesized as recently reported *(4)* and administered as an intravenous bolus (median 321, 290–360 MBq) a median 71 (66–79) min prior to the PET/CT. Patients underwent ^{18}F-rhPSMA-7.3 PET/CT on a Biograph mCT flow scanner (Siemens Medical Solutions, Erlangen, Germany) as recently described (*5,6*).

Patient Selection

The patients had received the injection of ^{18}F-rhPSMA-7.3 at various timepoints post-production and, consequently, had been administered different specific activities of ^{18}F-rhPSMA-7.3. The specific activity at the time of tracer injection was calculated for every patient using the exact time of injection, the injected activity and the radiolabeling quality control data for the particular batch, while accounting for the known radioactive decay of ^{18}F. Two patient groups were created (“high” or “low” specific activity) aiming for a 10-fold difference between groups. In

addition, groups were matched for uptake time and body weight and only patients with a low tumor load were included to avoid tumor sink effects. Low tumor load was defined as ≤1% of total injected dose accumulated in tumor lesions determined by isocontour volume of interest (VOI) measurements at 50% of the maximum standardized uptake value (SUV_{max}).

Biodistribution Assessment

SUV_{mean} were determined within standardized isocontour VOIs with 50% of the SUV_{max} and a diameter of 30mm, (salivary glands, liver, spleen, kidneys, bone, muscle, bloodpool, and tumor lesions). For evaluation of the tumor uptake, VOIs were placed over a maximum of 3 lesions per patient in decreasing order of the SUV_{max} and SUV_{mean} were averaged. The image-derived whole organ radioactivity concentration (kBq/mL) based on full organ segmentation salivary glands, liver, spleen and kidneys) was determined using semi-automatic analysis with the software qPSMA as previously described (*8*). VOI placement and image analyses were performed by two experienced nuclear medicine physicians.

Statistical Analysis

The Mann-Whitney U-Test was used to test for differences between uptake parameters between the “high” and the “low” specific activity groups. Additionally, a multivariate analysis (one-way MANOVA) was performed to analyze the effect of specific activities on biodistribution. Normal distribution of variables was evaluated by Q-Q plots and the Shapiro-Wilk W test. Data are presented as median (interquartile range), a *P*-value <0.05 was considered statistically significant. Statistical analysis was performed with SPSS Statistics, version 24 (IBM Corp., USA) and MedCalc, version 14.8.1 (MedCalc Software Ltd., Belgium).

RESULTS

Patient Population

From a total of 1975 patients, 84 cases were selected and stratified into two groups, each with 42 patients. The median time interval between tracer synthesis and injection was 72 (54–89) min vs. 367 (342–397) min for the “high” and “low” group (P<0.001), resulting in a median specific activity of ^{18}F-rhPSMA-7.3 of 178.9 (158.6–199.1) and 19.3 (17.7–22.5) MBq/µg, respectively (P<0.001). Median injected activity per bodyweight (4.0 [3.9–4.0] vs. 4.0 [3.9–4.0] MBq/kg) and median ^{18}F-rhPSMA-7.3 uptake time (70 [65–76] vs. 75 [68–87] min) were similar in the “high” and “low” group (P=0.62 and 0.06, respectively). No substantial differences between the groups were present for any clinical parameter (Supplementary Table 1). Supplementary Table 2 provides data for specific activities at calibration and injection.

Normal Organ Biodistribution and Tumor Lesions Evaluated by SUV_{mean}

Median SUV_{mean} in the “low” specific activity group were significantly lower for parotid glands (P=0.014), submandibular glands (P=0.002) and spleen (P =0.012) (Figure 1; Supplementary Table 3). No significant differences in SUV_{mean} were found for the other investigated organs. Median SUV_{mean} were 9.0 (4.4–14.8) and 9.5 (6.5–19.0) for tumor lesions in the “high” vs. “low” specific activity groups, respectively, and not significantly different (P=0.273). No statistical difference was observed for tumor lesion distribution between both groups (Supplementary Figure 2).

Whole Organ Radioactivity Concentrations

Whole organ radioactivity concentrations for the “high” vs. “low” ^{18}F-rhPSMA-7.3 specific activity group were 39.6 (34.8–48.0) vs. 29.4 (26.5–37.0), 46.9 (38.9–58.1) vs. 35.8 (28.6–43.2), 15.7 (12.6–19.4) vs. 15.1 (12.4–17.5), 21.1 (18.4–28.1) vs. 16.5 (12.2–20.0) and 69.3 (60.0–78.6) vs. 64.6 (52.1–72.1) kBq/ml for the parotid glands, submandibular glands, liver, spleen and kidneys, respectively. Results for the “low” specific activity group were significantly lower for salivary glands and spleen (each $p<0.001$), while liver and kidneys did not show significant differences (Figure 2).

A multivariate analysis (one-way MANOVA) confirmed the statistically significant difference between the “high” and “low” specific activity group for tracer distribution determined by SUV_{mean} and full organ segmentation, as described above (combined dependent variables, $F(14, 60)=3.928$, $P<0.001$, partial $\eta^2=.478$, Wilk’s $\Lambda=.522$.)

DISCUSSION

In this retrospective analysis, we explored the impact of ^{18}F-rhPSMA-7.3 specific activity on biodistribution in normal organs and tumors. Our data show that uptake patterns in organs relevant to clinical imaging interpretation are not substantially affected by different specific activities, with only the salivary glands and spleen demonstrating a moderate, albeit significant decrease in the low compared with high specific activity group. Tumor uptake appeared stable over the 10-fold difference investigated. Our results indicate that clinical PET interpretation is not affected using a single large batch production over several hours during the workday and the resultant wide range of injected specific activities.

Similar effects have already been demonstrated by Soeda et al. in a preclinical setting (*7*). In a mouse xenograft model derived from human lymph node metastases, a substantial decline in the SUV_{mean} of tumor lesions and salivary glands were observed on ^{18}F-PSMA-1007 PET/CT when reducing the molar activity over a 100-fold range (*7*). Despite decreased tumor uptake, the tumor-to-salivary gland ratio increased as salivary gland uptake was even further reduced compared with tumors. The authors concluded that this might play a role in reducing off-target uptake of PSMA-targeting radioligand therapies. Comparable findings have been demonstrated with ^{68}Ga-labeled PSMA inhibitors using triazacyclononane-triphosphinate chelators (*9*). By adding unlabeled compounds, the accumulation in the kidneys and salivary glands was altered significantly but less so in the tumor, with a more beneficial kidney-to-tumor ratio in lower molar activities of 8 vs. 1200 MBq/nmol (*9*).

To translate these animal data into clinical context, two different methodologies for detection of imaging-derived biodistribution of ^{18}F-rhPSMA-7.3 were applied. Recently,

biodistribution of ^{18}F-rhPSMA-7.3 has been investigated in 6 healthy subjects, where ^{18}F-rhPSMA-7.3 showed high physiologic uptake in the kidneys and salivary glands (*10*). Our study demonstrated, that the uptake of most organs is not influenced by receiving lower specific activities as it might occur during clinical practice in a busy PET clinic. This appears essential for clinical PET/CT reading. Additionally, tumor uptake did not vary significantly, even with a 10-fold difference in the injected specific activity.

This difference in specific activity represents the realistic spectrum of what is observed in a real-world scenario for PET-imaging. Although some of the mentioned preclinical findings can also be observed in our investigation with significant effect, they appear to be without clinical relevance in case of the salivary gland and spleen uptake. Notably, as therapeutic applications usually require higher molar masses (approx. 50–200 µg) our data cannot be extrapolated to the potential therapeutic use of rhPSMA-7.3.

Results of our study indicate that salivary gland uptake is saturable, suggesting binding to a target protein within the salivary glands. Similar findings were shown in preclinical studies of ^{177}Lu-PSMA-617, for which the uptake in the salivary glands and kidneys in PC3-PIP tumor-bearing mice significantly declined without impact on tumor uptake when adding cold PSMA-11 (*11*).

Some limitations of our study should be considered, e.g. the retrospective design. However, we believe that our observations are true reflections of the variance in specific activity in daily clinical practice. Second, our cohort comprised a relatively heterogeneous patient group at different stages of prostate cancer. Nevertheless, we tried to control for potential influence on biodistribution selecting patients based on low tumor load. The heterogenous population and the

known high variance of *in vivo* PSMA-expression might explain the wide range of reported SUV_{mean} in tumor lesions.

In summary, our data suggest that a single production of ^{18}F-rhPSMA-7.3 can be used in a clinical setting throughout the whole working day without clinically relevant effect on biodistribution, especially tumor lesion uptake despite significantly decreasing specific activity. This observation underlines the potential logistical and economic advantages of ^{18}F-labelled PSMA-ligands resulting from a single large batch production in a cyclotron facility over generator-produced ^{68}Ga-based ligands with short half-life and need of multiple batches throughout the day (*12*).

CONCLUSION

Differences in the injected specific activity of ^{18}F-rhPSMA-7.3 observed throughout a usual working day have no clinically relevant effect on biodistribution and especially uptake of tumor lesions. These results support central production of ^{18}F-labeled PSMA ligands with shipment to PET clinics similar to ^{18}F-fluorodeoxyglucose.

DISCLOSURE

Patent application for rhPSMA (ME, AW, HJW). ME and WW are consultants for Blue Earth Diagnostics (licensee for rhPSMA).

ACKNOWLEDGEMENT

Editorial support was provided by Dr C Turnbull (Blue Earth Diagnostics).

KEY POINTS

Question: Does the specific activity of radiopharmaceutical administered to the patient affect the way it distributed among organs?

Pertinent Findings: This retrospective data review showed that while the salivary glands and spleen appear to be saturable with decreasing specific activities, there was no clinically meaningful difference in organ uptake in patients with prostate cancer.

Implications for patient care: A single batch of ^{18}F-rhPSMA-7.3 can be used throughout the day to scan multiple patients without any effect on image quality being observed between the first and last patient of the day.

REFERENCES

1. Dietlein M, Kobe C, Kuhnert G, et al. Comparison of [^{18}F]DCFPyL and [^{68}Ga]Ga-PSMA-HBED-CC for PSMA-PET imaging in patients with relapsed prostate cancer. *Mol Imaging Biol.* 2015;17:575–584.

2. Giesel FL, Hadaschik B, Cardinale J, et al. F-18 labelled PSMA-1007: biodistribution, radiation dosimetry and histopathological validation of tumor lesions in prostate cancer patients. *Eur J Nucl Med Mol Imaging.* 2017;44:678–688.

3. Werner RA, Derlin T, Lapa C, et al. ^{18}F-Labeled, PSMA-targeted radiotracers: Leveraging the advantages of radiofluorination for prostate cancer molecular imaging. *Theranostics.* 2020;10:1–16.

4. Wurzer A, DiCarlo D, Schmidt A, et al. Radiohybrid ligands: a novel tracer concept exemplified by ^{18}F- or ^{68}Ga-labeled rhPSMA-inhibitors. *J Nuc Med.* 2019;61:735–742.

5. Eiber M, Kronke M, Wurzer A, et al. ^{18}F-rhPSMA-7 positron emission tomography for the detection of biochemical recurrence of prostate cancer following radical prostatectomy. *J Nuc Med.* 2019;61:696–701.

6. Kronke M, Wurzer A, Schwamborn K, et al. Histologically-confirmed diagnostic efficacy of ^{18}F-rhPSMA-7 positron emission tomography for N-staging of patients with primary high risk prostate cancer. *J Nuc Med.* 2019;61:710–715.

7. Soeda F, Watabe T, Naka S, et al. Impact of ^{18}F-PSMA-1007 uptake in prostate cancer using different peptide concentrations: Preclinical PET/CT study on mice. *J Nucl Med.* 2019;60:1594–1599.

8. Gafita A, Bieth M, Kronke M, et al. qPSMA: Semiautomatic software for whole-body tumor burden assessment in rostate cancer using ^{68}Ga-PSMA11 PET/CT. *J Nucl Med.* 2019;60:1277–1283.

9. Wurzer A, Pollmann J, Schmidt A, Reich D, Wester HJ, Notni J. Molar activity of Ga-68 labeled PSMA inhibitor conjugates determines PET imaging results. *Mol Pharm.* 2018;15:4296–4302.

10. Tolvanen T, Kalliokoski KK, Malaspina S, et al. Safety, biodistribution and radiation dosimetry of ^{18}F-rhPSMA-7.3 in healthy adult volunteers. *J Nucl Med.* 2021;62:679–684.

11. Kalidindi TM, Lee SG, Jou K, et al. A simple strategy to reduce the salivary gland and kidney uptake of PSMA-targeting small molecule radiopharmaceuticals. *Eur J Nucl Med Mol Imaging.* 2021 [Epub ahead of print].

12. Kesch C, Kratochwil C, Mier W, Kopka K, Giesel FL. ^{68}Ga or ^{18}F for prostate cancer imaging? *J Nucl Med.* 2017;58:687–688.

240 **FIGURE LEGENDS**

241

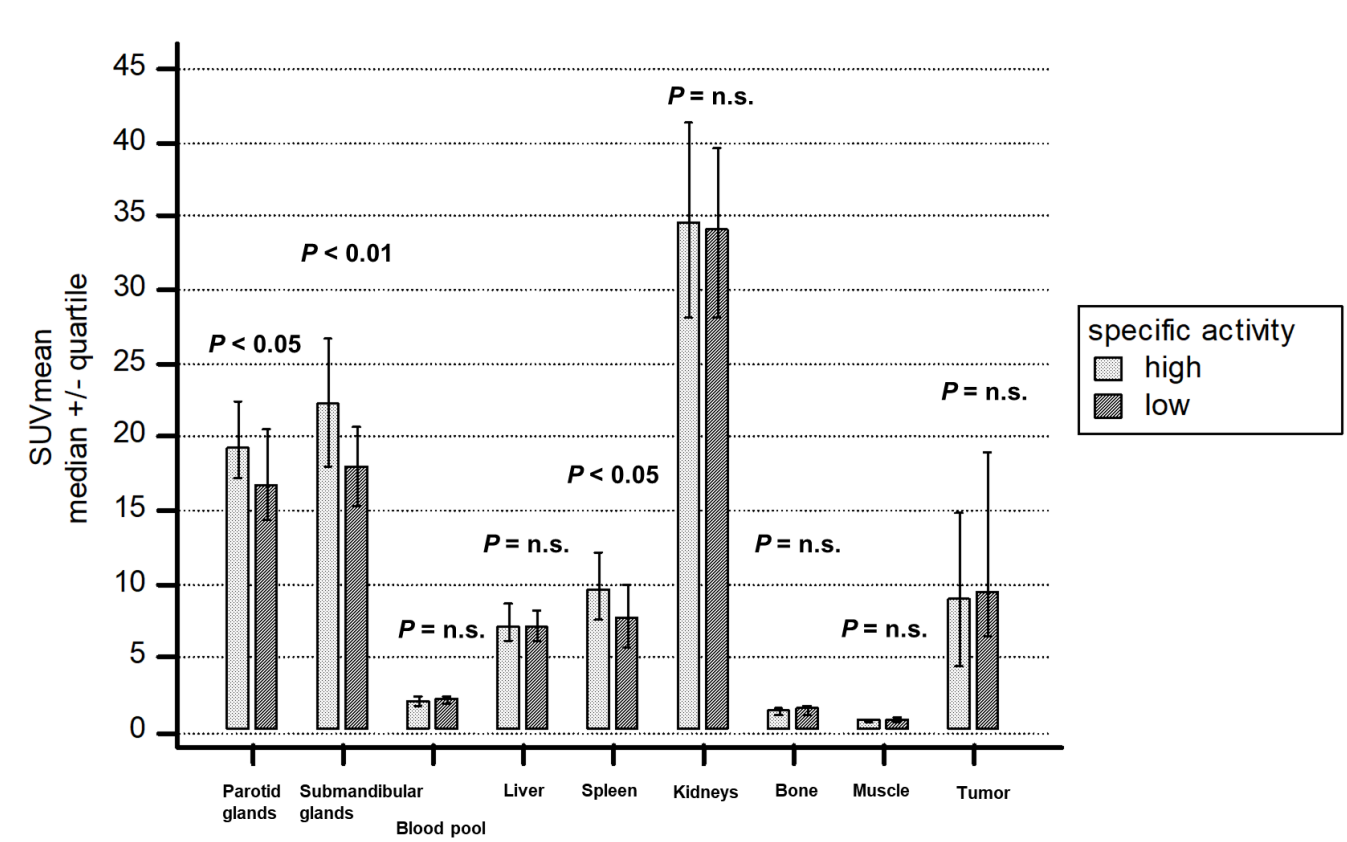

242

243 **FIGURE 1** ^{18}F-rhPSMA-7.3 SUV_{mean} stratified by injected specific activity

244

245

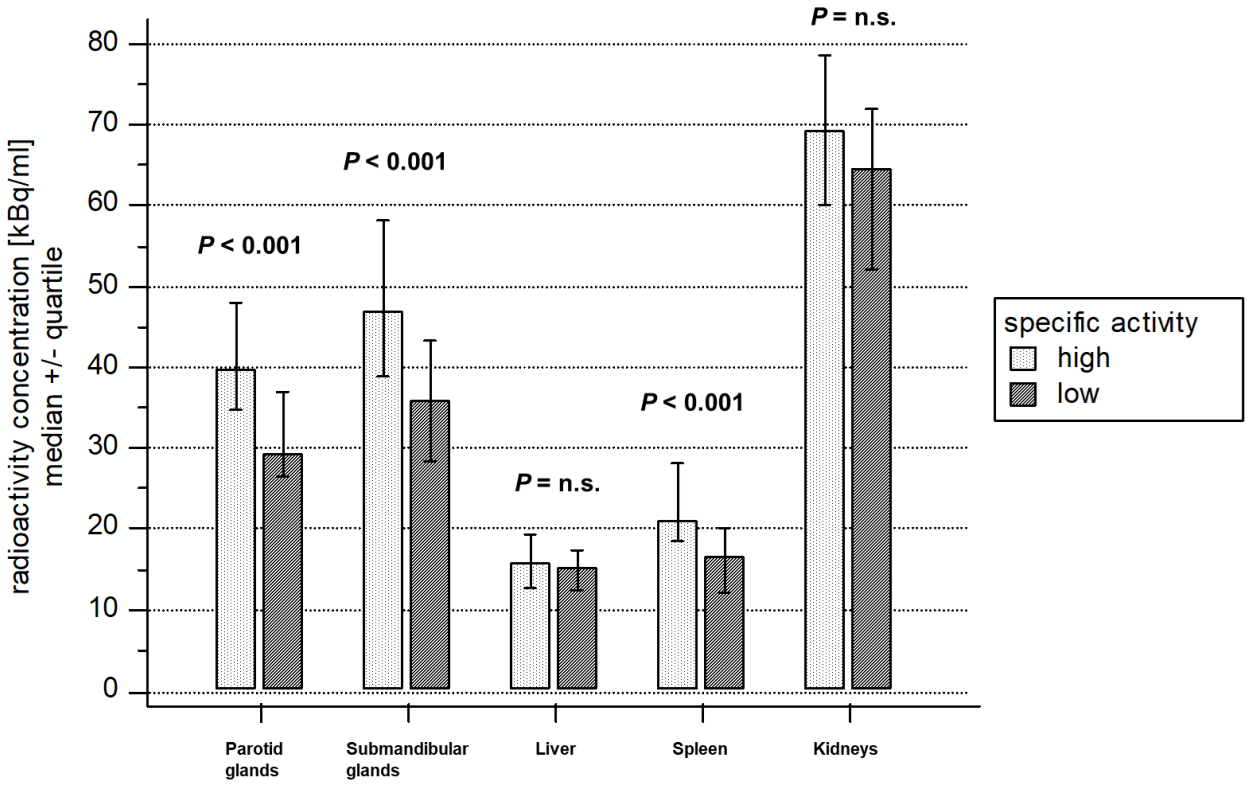

246

247 **FIGURE 2** ^{18}F-rhPSMA-7.3 whole organ radioactivity concentration stratified by injected

248 specific activity

249

250 **GRAPHICAL ABSTRACT**

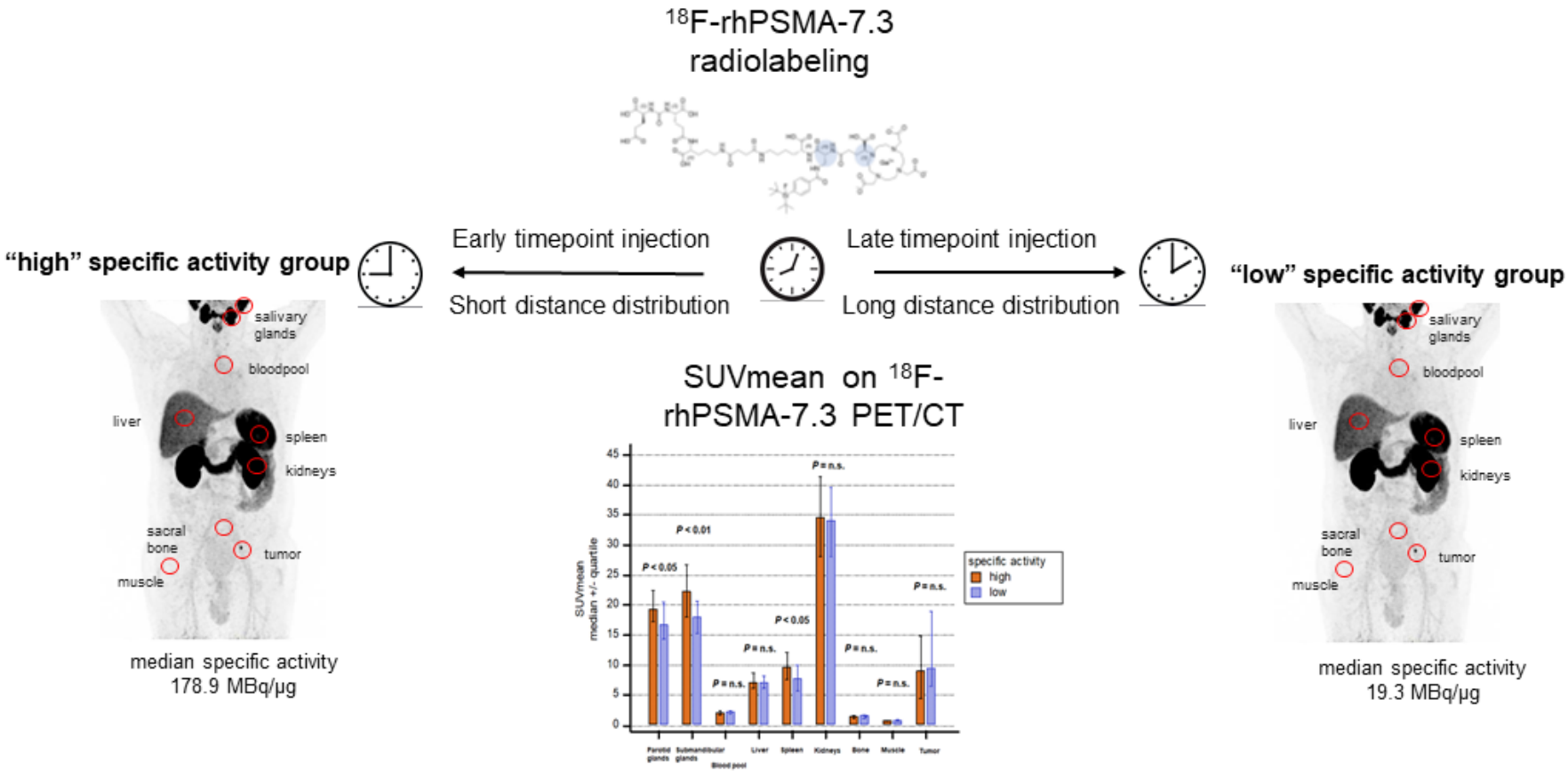

251

TABLES

	Total population (n=84)	"high" specific activity group (n=42)	"low" specific activity group (n=42)	*P* value *
Median (interquartile range) age in years	71.5 (64–77.5)	69.5 (63–77)	72 (65–78)	*P* = 0.3183
Median (interquartile range) ISUP grade	3 (2–5)	3 (2–4)	3 (2–5)	*P* = 0.3540
Median (interquartile range) PSA at timepoint of scan (ng/mL)	2.67 (0.55–11.42)	2.40 (0.55–9.13)	3.99 (0.53–14.80)	*P* = 0.2138
ADT in the 6 months prior to PET/CT	35/84 (41.7%)	19/42 (45.2%)	16/42 (38.1%)	*P* = 0.6580
Indication for PET/CT				*P* = 0.4227
Primary staging	18 (21.4%)	9 (21.4%)	9 (21.4%)	
Restaging of biochemical recurrence	45 (53.6%)	20 (47.6%)	25 (59.5%)	
Metastasized prostate cancer	21 (25.0%)	13 (31.0%)	8 (19.0%)	
Median (interquartile range) injected activity per bodyweight (MBq/kg)	4.0 (3.9–4.0)	4.0 (3.9–4.0)	4.0 (3.9–4.0)	*P* = 0.6176
Median (interquartile range) ^{18}F-rhPSMA-7.3 uptake time (minutes)	71 (66–79)	70 (65–76)	75 (68–87)	*P* = 0.0602
Median (interquartile range) specific activity (MBq/µg)	81.4 (19.3–178.9)	178.9 (158.6–199.1)	19.3 (17.7–22.5)	*P* < 0.0001

Supplementary Table 1 Patient characteristics stratified by "high" vs. "low" specific activity group. Clinical and PET parameters were matched for both groups. median specific activity at time point of injection was different by a factor of 10 ($P<0.0001$).

ADT. androgen deprivation therapy; ISUP. International Society of Urological Pathology; PET/CT. positron emission tomography/computed tomography; PSA. prostate specific antigen. * *Mann-Whitney U test*

	Patients injected with	
	"high" specific activity	**"low" specific activity**
Specific activity at calibration [MBq/µg] median (IQR)	281.3 (247.1-346.6)	197.8 (181.6-237.8)
Time between calibration and injection [min] median (IQR)	72 (54-89)	367 (342-397)
Specific activity at injection [MBq/µg] median (IQR)	178.9 (158.6–199.1)	19.3 (17.7–22.5)
Proportion of ^{18}F-labelled rhPSMA-7.3 [%] * median (IQR)	0.69 (0.60-0.84)	0.48 (0.44-0.58)
injected mass [µg] median (IQR)	1.75 (1.61-1.83)	17.43 (15.27-19.96)

Supplementary Table 2 Data for specific activity at calibration, time between calibration and patient injection, specific activity at injection and injected mass for the “high” and “low” specific activity group.

Organ	"high" specific activity Median SUV_{mean} (interquartile range)	"low" specific activity Median SUV_{mean} (interquartile range)	*P*
Parotid glands	19.2 (17.2–22.4)	16.7 (14.4–20.5)	*P*=0.0142
Submandibular glands	22.3 (18.0–26.7)	18.1 (15.2–20.6)	*P*=0.0017
Bloodpool	2.0 (1.8–2.3)	2.2 (1.9–2.4)	*P*=0.1591
Liver	7.2 (6.1–8.7)	7.1 (6.2–8.2)	*P*=0.9929
Spleen	9.6 (7.7–12.2)	7.8 (5.7–10.0)	*P*=0.0115
Kidneys	34.5 (28.1–41.3)	34.2 (28.1–39.7)	*P*=0.8650
Bone	1.4 (1.1–1.6)	1.5 (1.1–1.8)	*P*=0.2128
Muscle	0.8 (0.7–0.8)	0.8 (0.7–0.9)	*P*=0.7051
Tumor	9.0 (4.4–14.8)	9.5 (6.5–19.0)	*P*=0.2734

Supplementary Table 3 ^{18}F-rhPSMA-7.3 SUV_{mean} stratified by ^{18}F-rhPSMA-7.3 specific activity (volume of interest analysis)

FIGURES

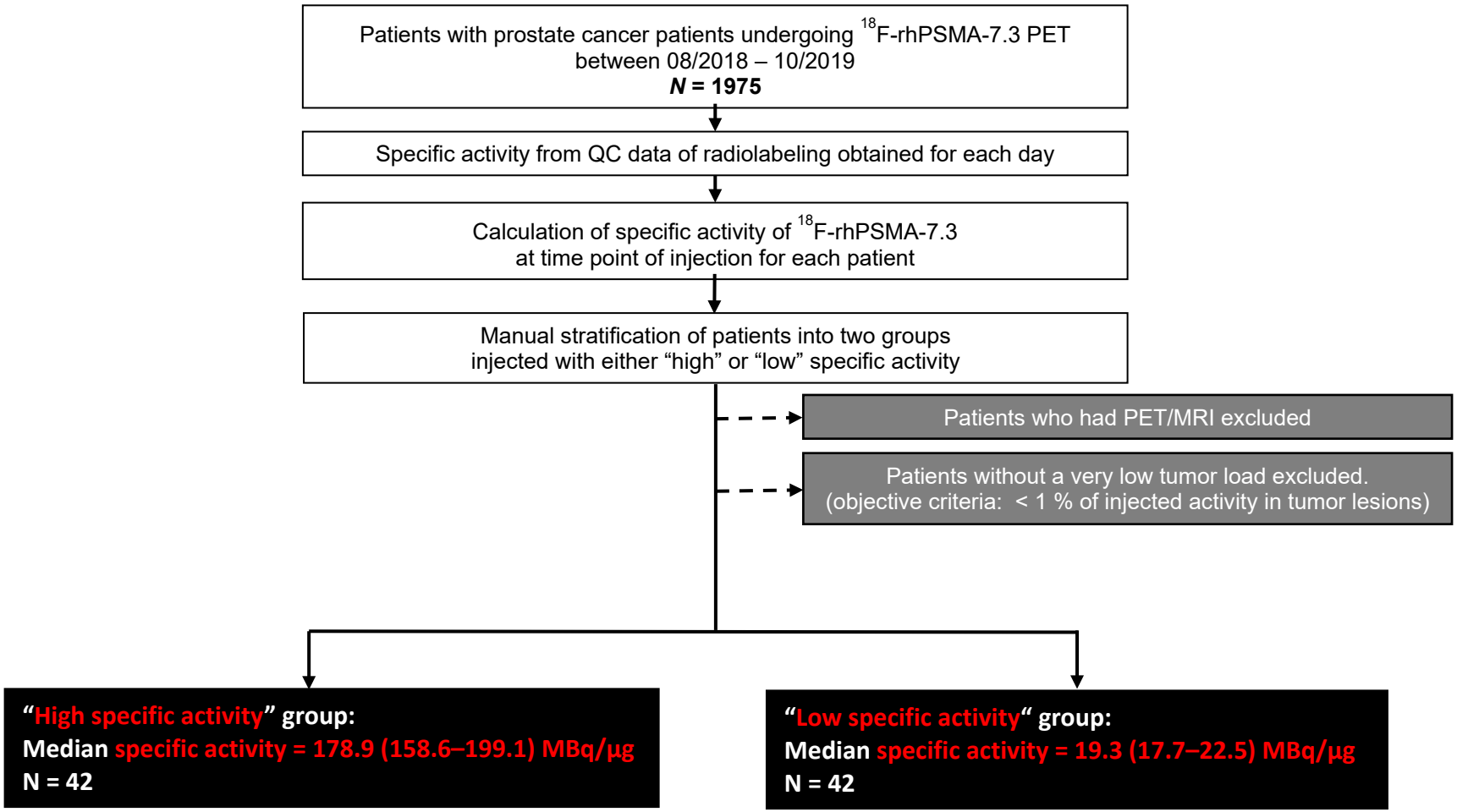

Supplementary Figure 1 Study flow chart

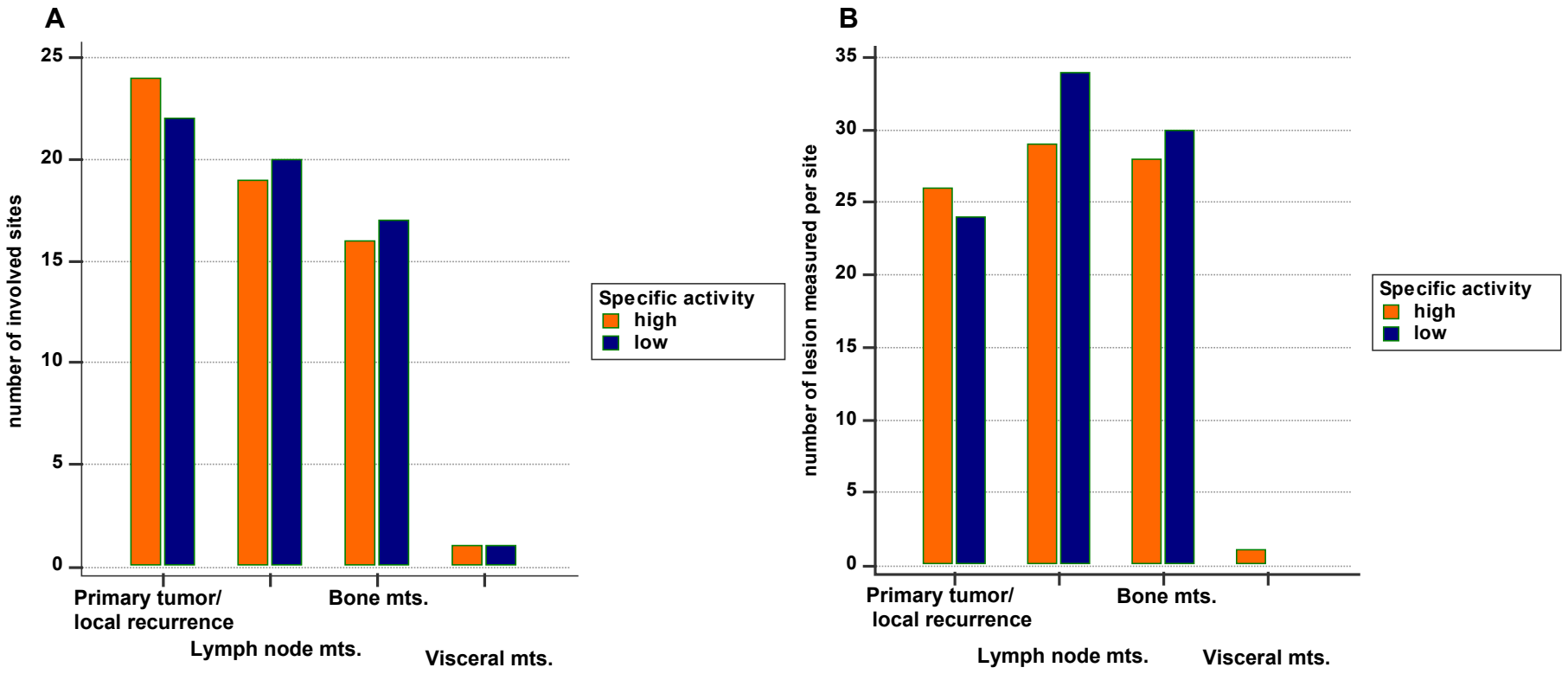

Supplementary Figure 2 Number and localization of the analyzed tumor lesion compared for both groups. No statistical difference of the lesion distribution was present between the "high" and "low" specific activity group. A: type and number of tumor sites involved in the patient cohorts

B: types and number of tumor lesions included in the quantitative SUV-based analysis. Mts. = metastases.